Case Studies in Thermal Engineering 45 (2023) 102967

Contents lists available at ScienceDirect

Case Studies in Thermal Engineering

journal homepage: www.elsevier.com/locate/csite

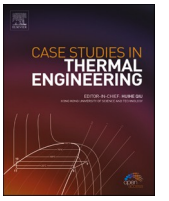

Improving the performance of a commercial absorption cooling system by using ejector: A theoretical study

Hamza K. Mukhtar *, Saud Ghani

Department of Mechanical and Industrial Engineering, Qatar University, P.O. Box 2713, Doha, Qatar

HIGHLIGHTS

- The integration of an ejector with the Robur absorption cooling system (RACS) improved the COP by 70.6% and decreased the required circulation ratio (CR) by 41% on average.
- The increase in the ambient temperature not only increases the activation temperature, but also decreases the COP and increases the circulation ratio (CR).
- Lowering the evaporator temperature is recommended in hot environments to avoid the need for high CR.
- Optimizing the ejector by reducing the throat diameter and increasing the mixing-tube diameter enhances the cooling system performance as long as the ejector operates under critical conditions.
- Among the three characteristic heat recovery coils in the RACS, it was found that the absorber coil had the most significant impact on the cooling performance.

ARTICLE INFO

Keywords:
Absorption cooling
Cooling system
Ammonia-water
Robur chiller
Ejector

ABSTRACT

Absorption cooling systems (ACS) have lower coefficients of performance (COP) compared to direct expansion (DX) cooling systems. Nevertheless, ACS offers a green alternative to typical DX systems. In this study, a numerical model was developed for the commercial low-capacity Robur® absorption cooling system (RACS). The model was developed based on mass, concentration, and energy balance equations, in addition to heat transfer equations. The model results were validated against experimental data available in the literature for the same cooling unit yielding a good agreement. Hence, to improve the COP of the RACS, a vapor ejector was introduced between the generator and the condenser. An improvement of 70.6% in the COP was obtained at the design condition. A parametric analysis was implemented to study the significance of the key parameters in the RACS performance. It was found that the increase in the ambient temperature not only increased the activation temperature, but it also decreased the COP and increased the circulation ratio (CR). Consequently, in hot environments, lowering the evaporator temperature is recommended to avoid the need for higher CR. Optimizing the nozzle throat and the mixing tube diameter improves the ejector performance, and hence the RACS performance, as long as the ejector operates under critical conditions. Finally, the absorber coil was found to have the most significance on the RACS performance in comparison with the rectifier coil and the refrigerant heat exchanger.

* Corresponding author.
E-mail address: Hmukhtar@qu.edu.qa (H.K. Mukhtar).

https://doi.org/10.1016/j.csite.2023.102967
Received 13 February 2023; Received in revised form 26 March 2023; Accepted 29 March 2023
Available online 31 March 2023

Nomenclature

ACS	Absorption cooling system
CACS	Conventional absorption cooling system
COP	Coefficient of performance
C_P	Specific heat capacity at constant pressure
CR	Circulation ratio
D	Diameter
h	Enthalpy
HEACS	Hybrid ejector absorption cooling system
M	Mach number
P	Pressure
$\dot{Q}$	Heat rate
R	Gas constant
RACS	ROBUR® absorption cooling system
T	Temperature
x	Ammonia concentration
$\dot{W}$	Work rate
ϵ	Effectiveness of heat exchanger
$\dot{m}$	Mass flow rate
γ	Isentropic index
φ	Isentropic efficiency
ω_v	Entrainment ratio of the vapor ejector
η	Efficiency

Subscripts

a	Absorber
abC	Absorber's Coil
Ahea	Absorber air heat exchanger
amb	Ambient
c	Condenser
c_{in}	Inlet flow of the cold fluid
c_{out}	Outlet flow of the cold fluid
e	Evaporator
Ej	Ejector
el	Electrical
ex	Exit
g	Generator
h_{in}	Inlet of the hot fluid
in	Inlet
out	Outlet
p	Pump
pf	Primary fluid
re	Rectifier
reC	Rectifier coil
sf	Secondary fluid
t	Throat

1. Introduction

Absorption cooling systems (ACS) play a crucial role in meeting the cooling needs of residential, commercial, and industrial sectors, particularly in regions with hot and humid climates [1]. Nevertheless, there are several reasons for the downturn in the market of the low capacity ACS compared to the market of direct expansion (DX) cooling systems. For instance, the low COP of the commercially available absorption chillers, the large occupied space, the high initial cost, and the lack of mass production [2]. In turn, the growing demand for cooling, the aggravating global warming, and the need for climate change mitigation have led to a surge in the adoption of ACS. Given that ACS are environmentally friendly, the need for further improvement on the absorption chillers has emerged to compete with DX chillers in the market of low-capacity cooling systems.

To address the limitations of current absorption cooling technology, there is a need for research and improvement in various areas,

▪ According to Weber et al. [10] A COP between 0.53 and 0.58 can be achieved using linear Fresnel collectors on summer days. However, a high driving temperature of around 180 °C was required; which might seem economically infeasible.

❖ Increasing the number of equivalent separation stages improves the refrigerant purification process [3], which in turn improves the evaporator performance. Yet, too many separation stages increase the pressure drop in the generator. Thus, optimization should be done.

▪ Increasing the absorbent content enhances the absorption of the NH_3 even at lower pressures [7]. Nonetheless, the desorption process might be negatively affected because a higher concentration of the absorbent might exist in the generator. Further investigation is recommended.

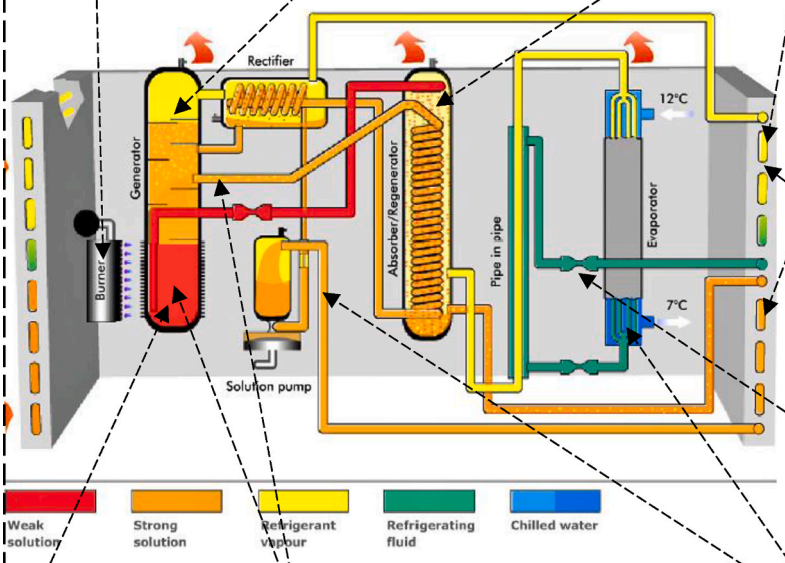

▪ In some water-cooled ACS, the condenser and the absorber are cooled in series by the same coolant. Horuz and Callander [6] recommended using a lower coolant temperature in the condenser than in the absorber.

▪ The use of water-cooled condensers and absorbers extends the range of possible operating conditions [6]. However, it aggravates the space occupied by the system.

❖ According to the simulation results of Darwish et al. [3], additional throttling valve has no significant effect on the COP.

▪ To prevent the sudden store-out of the mixture, adding a control strategy is recommended [7]. Simple flow-control sensors might be integrated into the pump-generator-heat source loop.

❖ Throttling the strong solution before it enters the generator flashes part of the solution Hence, it enhances the desorption process and increases the refrigerant mass flow rate. But the throttling process will reduce the high pressure of the cycle which in turn affects the liquefaction of the refrigerant before the evaporator [3]. Adding a flash tank to the cycle can resolve this issue.

▪ Enhancement of the heat transfer processes in the cycle improves the COP. Also, enhancing the heat transfer process in the evaporator at too-low cooling temperatures prevents the consequences of the low pressures downstream the pump (cavitation) [7].

▪ Experimental study ❖ Numerical Simulation (using Aspen Plus)

Fig. 1. Schematic diagram of some developments on RACS (ROBUR®).

such as materials, heat and mass transfer, and system design. For instance, enhancing the performance and efficiency of absorber and generator units [3], improving the heat and mass transfer processes in the evaporator and the condenser [4]. Moreover, optimizing system configurations and operation strategies [5] can significantly enhance the overall performance of absorption cooling systems.

1.1. Robur® absorption cooling system (RACS) in the literature

Various theoretical and experimental studies on commercial Robur absorption chillers were conducted. Darwish et al. [3] analyzed the performance of a 17.6 kW Robur absorption refrigeration system using Aspen Plus software. The simulation results revealed an acceptable agreement with the experimental data as reported by Horuz and Callander [6]. Nevertheless, a poor agreement was recorded against the manufacturer data as presented by Lazzarin et al. [7]. The deviation was attributed to the difference in the evaporator operating conditions. The performance of the distillation column represented by the number of equivalent mass transfer stages was investigated. The results showed that a design of 5 stages distillation column was the optimum with a 15% increase in the COP. To further improve the performance of the distillation column (the upper part of the desorber), two modifications were proposed. Firstly, flashing the strong solution entering the generator through a throttling process to boost the liberation of the refrigerant from the mixture. However, this process reduces the higher pressure in the cycle, which eventually reduces the amount of liquefied refrigerant at the evaporator inlet. Thus, the implementation of the throttling process seems unpractical, and experimental investigation is required to verify its feasibility. Secondly, injecting stripping inert gas to enhance heat and mass transfer, in addition to stripping more of the desired species "ammonia". However, the simulation result of this modification showed an insignificant increase of the system COP. To obtain more accurate thermos-physical properties of the ammonia-water mixture, Mansouri et al. [8] used a modified method from the Aspen-Plus library with fitted parameters. The Boston-Mathias modified Penge Robinson equations of state accurately predicted the vapor/liquid equilibrium for typical operating conditions of commercial absorption cooling systems. The developed model was validated, and then modified to allow the use of the overall heat transfer coefficient (UA) values as input parameters. The modified model was validated against experimental data from the literature yielding good agreement. The authors argued that the modified model predicted the properties of the mixture accurately, and it could be used to evaluate similar commercial chillers.

Experimentally, Lazzarin et al. [7] modified the composition of the antifreeze brine used in the evaporator to allow the 17.5 kW Robur chiller to produce refrigeration rather than cooling. The glycol concentration was increased from 35% to 55% in the chilled water. At constant heat input and pumping flow rate, the ammonia concentration in the generator decreased significantly when the outlet brine temperature decreased. Also, the refrigeration capacity decreased. Thus, to use such commercial chillers for refrigeration purposes some modifications should be implemented. For instance, the amount of the absorbent should be increased to ensure an efficient absorption process in the absorber. Overcooling of the condenser/absorber section should be avoided to prevent the drain-out of the solution in the generator. The heat transfer in the evaporator should be enhanced to alleviate the performance drop that occurs at very low pressures downstream the pump.

RACS demonstrated its feasibility to be integrated with solar systems. A. Haberle et al. [9] tested a linear concentrating Fresnel collector with a mirror area of 132 m^2 designed to drive a modified version of RACS in Bergamo, Italy. The two systems were connected via a water circuit pressurized up to 6 bar to provide a heat process of up to 200 °C. According to the data collected in the summer of 2007, the integrated system demonstrated a reliable operation. The solar system provided the RACS with heat at 180 °C with an efficiency of 40% with respect to direct normal irradiation. The integrated system operated stably for a year. Similarly, Weber et al. [10] carried out an operational investigation on the performance of two cascading rooftop 12 kW Robur absorption refrigeration chillers with rated COPs of 0.6. The heat input was provided at an average of 180 °C through linear Fresnel collectors with an aperture area of 132 m^2. The integrated system was designed for refrigeration purposes in cold rooms with ice storage units. The cascade layout was adopted to study the partial load operation. The integrated system was tested under different operation conditions in June 2006. The main results were related to the charging-discharging curve of the cold storage capacity. During the charging of the storage, the heat transfer decreased significantly due to ice build-up on the heat exchanger surface. Over a certain range of partial load, the combined system adjusted itself to a stable equilibrium temperature. However, the self-stabilization was limited by the maximum power of the chillers. The refrigeration effect and the COP increased with the driving temperature. The rated parameters of the chillers were obtained at an operating temperature of 200 °C. For representative summer days, the range of the COP was 0.53–0.58. It is noticeable that experimental investigations on absorption chillers were carried at heat source temperatures higher than those assumed in theoretical studies. This could be attributed to the fact that real-life ACSs encounter many losses and irreversibility counter to the theoretical studies that include several assumptions. Fig. 1 summarizes various modifications and developments found in the literature aiming to improve the RACS performance.

RACS performance is affected by several factors such as generator temperature, evaporator pressure, and the ambient temperature for air-cooled systems. Yet, there is a lack of a detailed analysis in the literature that shows how different operating parameters affect the performance of such chillers. While experimental investigation can provide a more accurate understanding of the RACS performance, it is associated with certain limitations such as technical complexities, time constraints, and high costs [6,7].Therefore, it is imperative to conduct theoretical investigations that can predict the system's behavior under different operating conditions and identify potential improvements, while mitigating these limitations.

In the present study, a theoretical model was developed to describe and analyze the operation and performance of an air-cooled RACS used for cooling purposes. A parametric study that included the major influential parameters such as generator temperature, evaporator pressure, ambient temperature, and ejector geometrical parameter was conducted. The system responses to the alternation of these parameters were depicted to identify the optimum conditions. The characteristic heat recovery processes of the RACS were analyzed.

To improve the RACS performance, the study further investigates adding an ejector to the RACS between the rectifier and the condenser. The ejector function is to utilize a high-pressure fluid to entrain a low-pressure fluid and to discharge the resultant mixture at an intermediate pressure.

2. System description before and after modification

RACS works on a thermodynamic cycle that differs from the basic absorption cooling cycle by heat recovery processes. The strong solution exiting from the solution pump undergoes two heat recovery processes in the rectifier and the absorber. Hence, the strong solution enters the generator at a temperature higher than that of the basic absorption cycle. Consequently, lower heat input is required, and a higher COP could be obtained.

The working principle of the Robur absorption cooling cycle is similar to the basic absorption cycle. Fig. 2(a) shows the schematic of the Robur absorption cooling system. After the purification process in the rectifier (Re), the ammonia vapor flows (Point 1) to the air-cooled condenser (C) in which it transfers heat to the surrounding. After the condensation process (Point 2), the pressure of the condensed refrigerant is reduced to the intermediate pressure (Point 3) when it passes through the expansion valve (EV-1). Then, it exchanges heat with the vapor ammonia that exits from the evaporator in the concentric refrigerant heat exchanger (RHE) (Point 4). Further decrease in the pressure occurs at the expansion valve-2 (EV-2). At (Point 5), the liquid ammonia is at appropriate conditions (low temperature and low pressure) to produce a cooling effect in the evaporator (E). The refrigerant is assumed to exit from the evaporator at a saturated vapor state (Point 6). Before it is drawn into the absorber (A), the saturated ammonia vapor absorbs more heat when it passes through the RHE (Point 7). Here, the low-pressure vapor ammonia is drawn by the weak solution that exists in the absorber where the exothermic absorption process begins. The resultant strong water/ammonia mixture (Point 8) is directed to the absorber-air-heat-exchanger (Ahea) to cool the mixture by the ambient air, and hence enhance the absorption of the ammonia in the mixture (Point 9). The pressure of the cool mixture is increased via a solution pump (SP) (Point 10). Before it enters the generator (G), a two-stage temperature rise is taken place for this mixture. The first temperature rise occurs in the rectifier coil (REC) (Point 11), whereas, the second temperature rise occurs in the absorber coil (ABC) (Point 12). Eventually, the strong water-ammonia mixture reaches the generator at relatively high temperature. In the generator, the solution is heated up through an external heat source (HS). As a result, part of the mixture with a significant high concentration of ammonia refrigerant evaporates, leaving behind a mixture with less amount of ammonia (weak solution) in comparison with the (strong solution) coming from the absorber. This weak solution leaves the generator (Point 13) and its pressure decreases as it passes through the expansion valve-3 (EV-3) (Point 14) before it flows back to the absorber to perform the absorption process. The high ammonia concentration mixture evaporated in the generator is directed to the rectifier for the purification process (Point 15). Two streams leave the rectifier, the first stream is a weak solution that returns to the generator (Point 16), and the second stream is the purified refrigerant that completes the cycle.

The performance of conventional absorption cooling systems (CACS) could be enhanced by using ejectors. The devices were added to the basic cycle in various locations to form different improved configurations of absorption cooling systems. Mukhtar and Ghani summarized recent studies on the combined ejector-absorption cooling systems, indicating that COPs of above unity could be achieved by single and dual ejector-absorption cooling systems [11].

In the present study, an ejector is added to the RACS between the rectifier and the condenser as shown in Fig. 2(b). Part of the refrigerant vapor exiting from the concentric RHE is entrained in the ejector (Ej) by the high-pressure refrigerant vapor from the rectifier. Whereas, the remaining refrigerant from the evaporator is absorbed by the weak solution in the absorber as in the original Robur absorption cooling system.

The ejector function is to utilize a high-pressure fluid to entrain a low-pressure fluid and to discharge the resultant mixture at an intermediate pressure. The ejector is either introduced between the generator and the condenser to form low-pressure-condenser (LPC) ACS, or placed at the entrance of the absorber to form Triple Pressure Level (TPL) ACS. The LPC-ACS is more common in the literature as it achieves higher COP improvement. Therefore, adding the ejector between the generator and the condenser in the RACS is

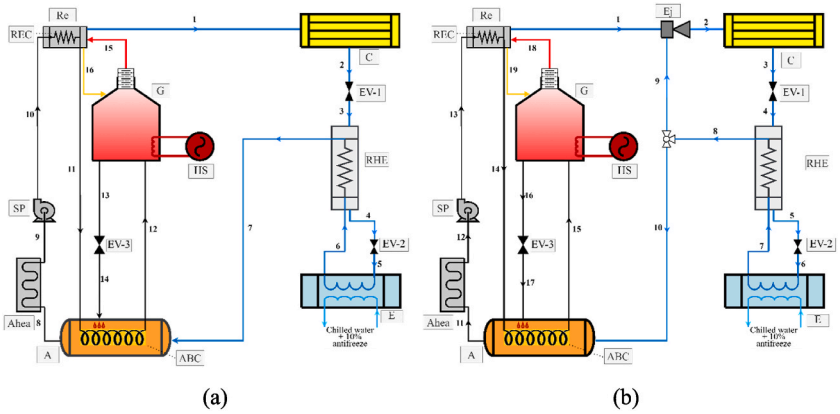

Fig. 2. A schematic of Robur absorption cooling system before and after adding an ejector.

proposed in the present study. The high-pressure refrigerant vapor leaving the rectifier is directed to the ejector as shown in Fig. 2(b). Subsequently, the vapor enters a convergent-divergent nozzle to convert part of its pressure into kinetic energy as revealed in the schematic of the pressure distribution inside the ejector shown Fig. 3. In the convergent section of the nozzle, the flow is subsonic and the Mach number (M) is less than unity. Accordingly, the velocity increases, while the pressure decreases. At best ejector operation scenario, the vapor flow is choked at the throat where (M) reaches the value of 1 (Point **t**), and the mass flow rate is maximum. At the divergent section of the nozzle, the flow is supersonic ($M > 1$). Thus, the velocity increases and the pressure decrease in an adiabatic expansion process. The vapor exits the nozzle to a chamber where the velocity reaches the peak, and the pressure becomes lower than the pressure of the secondary fluid (section 1). Hence, distinct low-pressure regions are created. As a result, the secondary fluid from the RHE is entrained into the suction chamber. The continuous primary stream downstream the nozzle collides with the entrained fluid inducing eddy currents in the section chamber as depicted in Fig. 3. Due to the high momentum in the axial direction, the primary fluid pushes a considerable portion of the entrained fluid into the constant area mixing tube (section 2).

Hence, a shock circle is initiated at the entrance of the constant area mixing tube [12]. It settles in the infinitesimal region between the high-momentum primary stream and the secondary stream that is entrained at the vicinity of the tube wall. Thereafter, the mixing process evolves at a constant pressure. In a well performing ejector, a normal shock wave takes place somewhere downstream the mixing-tube (section 3). The mixture undergoes a sudden and dramatic increase in static pressure, temperature, and density. In contrast, the velocity drops significantly and the flow becomes subsonic ($M < 1$). Then, these properties stabilize until the mixture reaches the exit diffuser (section 4). As the area increases in the diffuser, the pressure of the subsonic mixture is boosted. The diffuser recovers the pressure as it discharges the mixture at (section 5) with a pressure slightly higher than the back pressure (condenser pressure). Usually, slightly more than half of the total compression achieved in the ejector is obtained through the shock wave (section 3). The rest compression is obtained in the diffuser (between sections 4 and 5).

3. Mathematical modeling

3.1. RACS model

To develop a mathematical model for the RACS, each component in the system was considered as a control volume. The assumptions for modeling the RACS are.

- The system operates at steady state condition.
- The working solution is homogeneous in the whole system.
- Kinetic and potential energies are negligible in all system components.
- No heat loss to the ambient except in the condenser and the absorber air heat exchanger.
- Pressure drop is negligible within the system except in the expansion valves.
- Expansion processes in the expansion valves are isentropic.
- The operating temperature in the rectifier is 20 °C less than the generator temperature.
- Both the weak solution leaving the generator and the refrigerant exiting the condenser are at saturated liquid states.
- Ammonia vapor leaves the generator, the rectifier, and the evaporator at saturated state.
- The temperatures upstream the condenser and the AHEA are 4 °C above the ambient temperature [13].
- The refrigerant vapor exits the rectifier at a concentration of 0.998.

The system was modeled based on mass, concentration, and energy balances, in addition to other complementary equations such as heat exchanger equations as follows:

$$\sum \dot{m}_{in} = \sum \dot{m}_{out} \quad mass\ balance \tag{1}$$

$$\sum \dot{m}_{in} * x_{in} = \sum \dot{m}_{out} * x_{out} \quad concentration\ balance \tag{2}$$

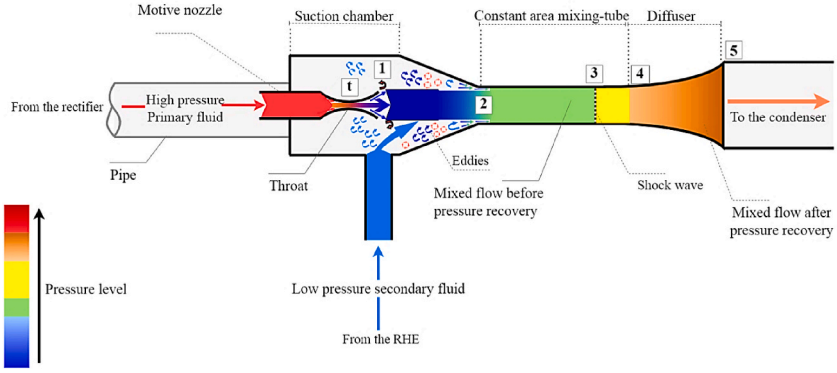

Fig. 3. Pressure distribution inside different sections of the vapor ejector.

$$\sum \dot{Q} + \sum \dot{m}_{in} * h_{in} = \sum \dot{W} + \sum \dot{m}_{out} * h_{out} \quad energy\ balance \tag{3}$$

$$\varepsilon = \frac{h_{c_{out}} - h_{c_{in}}}{h_{h_{in}} - h_{c_{in}}} \quad or \quad \varepsilon = \frac{T_{c_{out}} - T_{c_{in}}}{T_{h_{in}} - T_{c_{in}}} \quad effectiveness \tag{4}$$

$$COP = \frac{\dot{Q}_e}{\dot{Q}_g + \dot{W}_{in}} \quad where \quad \dot{W}_{in} = \dot{W}_p \Big/ \eta_{el} \quad Coefficient\ of\ performance \tag{5}$$

The design conditions input parameters of the cooling system are presented in Table 1.

The model was developed using EES built-in thermodynamics libraries and functions. Special Call-NH_3H_2O function was used to identify the thermodynamics properties of the ammonia-water mixture at each point in the cycle. It requires 3 input properties at each point to identify the rest 5 thermodynamics properties. Defining 3 properties at each point is unrealistic unless some assumptions are made.

On the other hand, the ejector was modeled based on the assumption of constant pressure mixing process. This assumption showed more accurate results compared to the assumption of constant area mixing process [14]. The flow inside the vapor ejector undergoes both chock and shock processes, hence, the ejector analysis becomes complex.

3.2. Ejector model

The geometrical parameters of the ejector have a significant influence on the ejector performance, and consequently the system performance. The design, operation, and analysis of the vapor ejector system are more complicated than the cooling system. The size of each area, as well as the nozzle shape and placement determine the ejector system performance. The nozzle design location is predominantly set by the manufacturer for specific design conditions. It plays an essential role in the ejector performance [15]. The most important event in vapor ejector operation is the occurrence of the shock wave that takes place when the ejector operates in the critical mode.

The refrigerant vapor flows through the ejector was treated as an ideal gas. The modeling of the ejector operation was carried according to the gas dynamics equations, in addition to the shock circle method as introduced by Zhu et al. [12].

Assumptions for the analysis of the ejector:

- The walls of the ejector are adiabatic.
- The ejector operates at critical mode operation.
- The kinetic energy of the two streams are negligible at the inlet sections.
- The primary fluid is uniformly distributed along the radial direction.
- The secondary flow is uniformly distributed in the suction chamber.
- The mixing process of the two streams occurs at constant pressure.
- The pressure and the temperature of the entrained fluid have uniform distribution along the radial direction.

At choke condition (M = 1):

$$\dot{m}_{pf} = P_{pf} . A_t . M_t \sqrt{\frac{\gamma \varphi_{pf}}{RT_{pr}}} . \left(\frac{2}{\gamma + 1}\right)^{\frac{\gamma+1}{2(\gamma-1)}} \quad primary\ fluid\ flow\ rate \tag{6}$$

Here P_{pf} and T_{pf} are the stagnation pressure and temperature of the primary fluid.

$$M_1 = \left(\frac{D_t}{D_1} . \left(\frac{2 + (\gamma - 1).M_1^2}{\gamma + 1}\right)^{\frac{\gamma+1}{4(\gamma-1)}}\right)^2 \quad Mach\ number\ at\ section\ 1 \tag{7}$$

$$T_{pf} = T_{pf_1} * \left[1 + \frac{(\gamma - 1)}{2} M_1^2\right] \quad temperature\ at\ section\ 1 \tag{8}$$

$$v_{pf_1} = M_1 \sqrt{\gamma R T_{pf_1}} \quad velocity\ at\ section\ 1 \tag{9}$$

$$p_2 = p_{sf} * \left[1 + \frac{(\gamma - 1)}{2} M_2^2\right]^{\frac{\gamma}{\gamma-1}} \quad pressure\ at\ section\ 2 \tag{10}$$

Table 1
Design operating conditions of the cooling system.

Parameter	T_g	T_e	T_{amb}	ε_{RHE}	ε_{abC}	ε_{reC}	η_p
Unit	°C	°C	°C	–	–	–	–
Value	100	5	30	0.8	0.6	0.6	0.98

$$T_2 = T_{pf} \Big/ \left[1 + \frac{(\gamma-1)}{2} M_2^2\right] \quad \textit{temperature at section 2} \tag{11}$$

$$v_{pf_2} = M_2 \sqrt{\gamma R T_{pf_2}} \quad \textit{centerline velocity at section 2} \tag{12}$$

$$D_{pf_2} = \frac{D_{pf_2}}{\sqrt{\varphi_{exp}}} \quad \textit{where } \varphi_{exp} = \varphi_{pf} . \varphi_{sf} \quad \textit{primary fluid diameter at section 2} \tag{13}$$

D_{pf_2} represents the actual diameter of the primary fluid at the entrance of the mixing tube.

$$D_{pf_2} = D_1 \, . \, \left(\frac{2 + (\gamma-1)M_2^2}{2 + (\gamma-1)M_1^2}\right)^{\frac{\gamma+1}{4(\gamma-1)}} \sqrt{\frac{M_1}{M_2}} \quad \textit{primary fluid actual diameter at section 2} \tag{14}$$

The exponential formula of the velocity in the shock circle between the two flows at section 2 is expressed as follows:

$$v_r = v_{pf_2} \left(1 - \frac{r}{R_2}\right)^{\frac{1}{n}} \quad \textit{velocity distribution at section 2} \tag{15}$$

$$n = \ln\left(1 - \frac{D_{pf_2}}{D_2}\right) \Big/ \ln\left(\frac{\sqrt{\frac{T_{sf_2}}{T_{pf_2}}}}{M_2}\right) \quad \textit{the exponential index} \tag{16}$$

The *average velocity* and *mass flow rate* of the secondary (entrained) fluid at section 2 are determined by the following formulas:

$$\overline{v}_{sf_2} = \frac{2 v_{pf_2}}{(D_2^2 - D_{pf_2}^{)}} \left[\frac{n D_2^2}{n+1}\left(1 - \frac{D_{pf_2}}{D_2}\right)^{\frac{n+1}{n}} - \frac{n D_2^2}{2n+1}\left(1 - \frac{D_{pf_2}}{D_2}\right)^{\frac{2n+1}{n}}\right] \tag{17}$$

$$\dot{m}_{sf} = \frac{\pi \, P_s v_{pf_2}}{2 \, R \, T_{sf_2}} \left[\frac{n D_2^2}{n+1}\left(1 - \frac{D_{pf_2}}{D_2}\right)^{\frac{n+1}{n}} - \frac{n D_2^2}{2n+1}\left(1 - \frac{D_{pf_2}}{D_2}\right)^{\frac{2n+1}{n}}\right] \tag{18}$$

The energy balance between the inlet and section 2 is expressed by the below equation:

$$\dot{m}_{pf} C_p T_{pf} + \dot{m}_{sf} C_p T_{sf} = \dot{m}_{pf} \left(C_p T_{pf_2} + {v_{pf_2}}^2/2\right) + \dot{m}_{sf} \left(C_p T_{sf_2} + {\overline{v}_{sf_2}}^2/2\right) + losses \tag{20}$$

where the losses could be evaluated through the following equation:

$$losses = \frac{1}{2}\dot{m}_{pf} v_{pf_1}^2 \left(1 - \varphi_{pf}\right) + \frac{1}{2}\dot{m}_{pf} v_{pf_2}^2 \left(1 - \varphi_{exp}\right) + \frac{1}{2}\dot{m}_{sf} \overline{v}_{sf_2}^2 \left(1 - \varphi_{sf}\right) \tag{21}$$

$$p_4 = p_2 * \left[1 + \frac{2\gamma}{\gamma+1}\left(M_2^2 - 1\right)\right] \quad \textit{pressure at sec tion 4} \tag{22}$$

$$M_4 = \sqrt{\frac{1 + \left(\frac{\gamma-1}{2}\right)M_2^2}{\gamma M_2^2 - \left(\frac{\gamma-1}{2}\right)}} \quad \textit{Mach number at section 4} \tag{23}$$

Design of the diffuser:

$$\frac{D_5}{D_4} = \left(\frac{2 + (\gamma-1)M_5^2}{2 + (\gamma-1)M_4^2}\right)^{\frac{\gamma+1}{4(\gamma-1)}} \cdot \sqrt{\frac{M_4}{M_5}} \quad \textit{Mach number at section 5} \tag{24}$$

The value of the M_5 should be as the smallest as possible, to the limit that just tolerates the flow to circulate across the condenser.

$$p_{4_0} = p_4 \left[1 + \frac{(\gamma-1)}{2} M_4^2\right] \quad \textit{Stagnation pressure at 4} \tag{25}$$

$$p_5 = p_{4_0} \Big/ \left[1 + \left(\frac{\gamma-1}{2}\right) M_5^2\right]^{\frac{\gamma}{\gamma-1}} \quad \textit{pressure at section 5} \tag{26}$$

The value of P_5 should be slightly higher than the condenser pressure. The maximum designed pressure (P*) at section 5 is limited to 1% higher than the condenser pressure.

Equations of the ejector performance:

$$\omega_v = \frac{\dot{m}_{sf}}{\dot{m}_{pf}} \quad entrainment\ ratio \tag{27}$$

$$Cr = \frac{P_5}{P_{sf}} \quad compression\ ratio \tag{28}$$

$$Er = \frac{P_{pf}}{P_{sf}} \quad expansion\ ratio \tag{29}$$

The ejector geometrical parameters, input parameters and constants are illustrated in Table 2. These values were set in accordance with the study of Khalili and Farshi [16]. Fig. 4 illustrates the solution algorithms of the two developed mathematical models. Namely, the solution algorithm and the ejector numerical model.

4. Results of the numerical model

4.1. Validation of the RACS numerical model

The model was validated against the experimental and theoretical data provided by Araujo et al. [17]. Considering the same operating conditions ($T_g = 399.65$ K, $T_e = 281.85$ K, $T_{amb} = 304.65$ K), the comparison was carried out for the temperature at 16 points of the basic system. A good agreement was obtained against the experimental data of Araujo et al. [17]. Excluding (Point 7), the maximum deviation of the current model results from the experimental data didn't exceed 7.7%. As indicated in Table 3, the outlier value was obtained at the exit of the concentric heat exchanger (Point 7). The temperature obtained by the present theoretical model in this location differed from the experimental value by 12.5%. However, the authors believe that the experimental value of the temperature at (Point 7) is unreasonable. At the cold side of the heat exchanger (Point 7), the refrigerant vapor is technically supposed to exit at a temperature higher than the inlet temperature (Point 6). However, the experimental data showed a lower temperature at (Point 7), which might imply a malfunctioning of the heat exchanger, temperature sensor or more probably an error in the recorded values.

4.2. Results and discussion

The coefficient of performance (COP) and circulation ratio (CR) were the main performance parameters considered in the analysis. The former reflects the technical performance, whereas the latter is associated with the physical size of the system. The main independent parameters that govern the system performance are generator temperature (T_g), and evaporator pressure (P_e). In addition, since the RACS is an air cooled system, hence, the ambient temperature (T_{amb}) plays an important role in the system's performance.

Theoretically, single-effect ACS operates at generator temperatures in the range of 80–120 °C. However, it is practically operated at higher temperatures that reach over 170 °C due to various losses and irreversibility within the system [9]. Accordingly, the system performance is investigated in the present study at a generator temperature of up to 170 °C.

In a basic ACS, the COP increases with the increase in the generator temperature. However, the increment rate decreases gradually until it nearly approaches zero at high temperatures. Under operating conditions of ($T_{amb} = 30$ °C, and $T_g > 140$ °C), the COP of the basic RACS stabilizes at approximately 0.54 as shown in Fig. 5. A similar behavior was obtained in the RACS with an ejector except that the increment rate in the COP with the generator temperature was significantly higher. Under the same operating conditions, the RACS with an ejector achieved a COP of over 0.95.

The system developed COP and the generator temperature are closely related to the activation temperature. The activation temperature is the minimum generator temperature required to operate the system. The activation temperature at each ambient temperature is revealed at the start of each corresponding curve in Fig. 5. Not only the increase in the ambient temperature decreases the COP, but it also increases the activation temperature of the system. It is an undesirable consequence, particularly when a low grade temperature source is used to drive the system.

The circulation ratio (CR) is defined as the ratio of the solution flow rate delivered by the pump to the refrigerant flow rate inside the evaporator. It indicates how much flow rate of the strong solution should be pumped to a generator operating at particular conditions to produce one unit of refrigerant mass flow rate at the evaporator. It is a design parameter that affects the system size and performance. The lesser the CR the better the performance, and the smaller the occupied space by the system. A typical trend was obtained by the current model for RACS. Fig. 6(a) shows the comparison in CR between the RACS with and without the ejector, whereas, Fig. 6(b) shows the change of the CR with the generator temperature under different ambient temperatures in the modified RACS.

The use of the ejector reduces the required CR by 41% on average. The enhancement is due to the entrained vapor in the ejector that leads to a higher mass flow rate at the evaporator compared to the system without the ejector.

At the activation temperature of the system, the CR is high because the system is barely capable to vaporize an adequate part of the

Table 2
Design operating conditions of the ejector.

Parameter	D_t	D_1	D_2	φ_{pf}	φ_{sf}	γ	C_p	R
Unit	mm	mm	mm	%	%	–	kJ/kg.K	kJ/kg.K
Value	3	4.5	6	95	85	1.32	2.185	0.4882

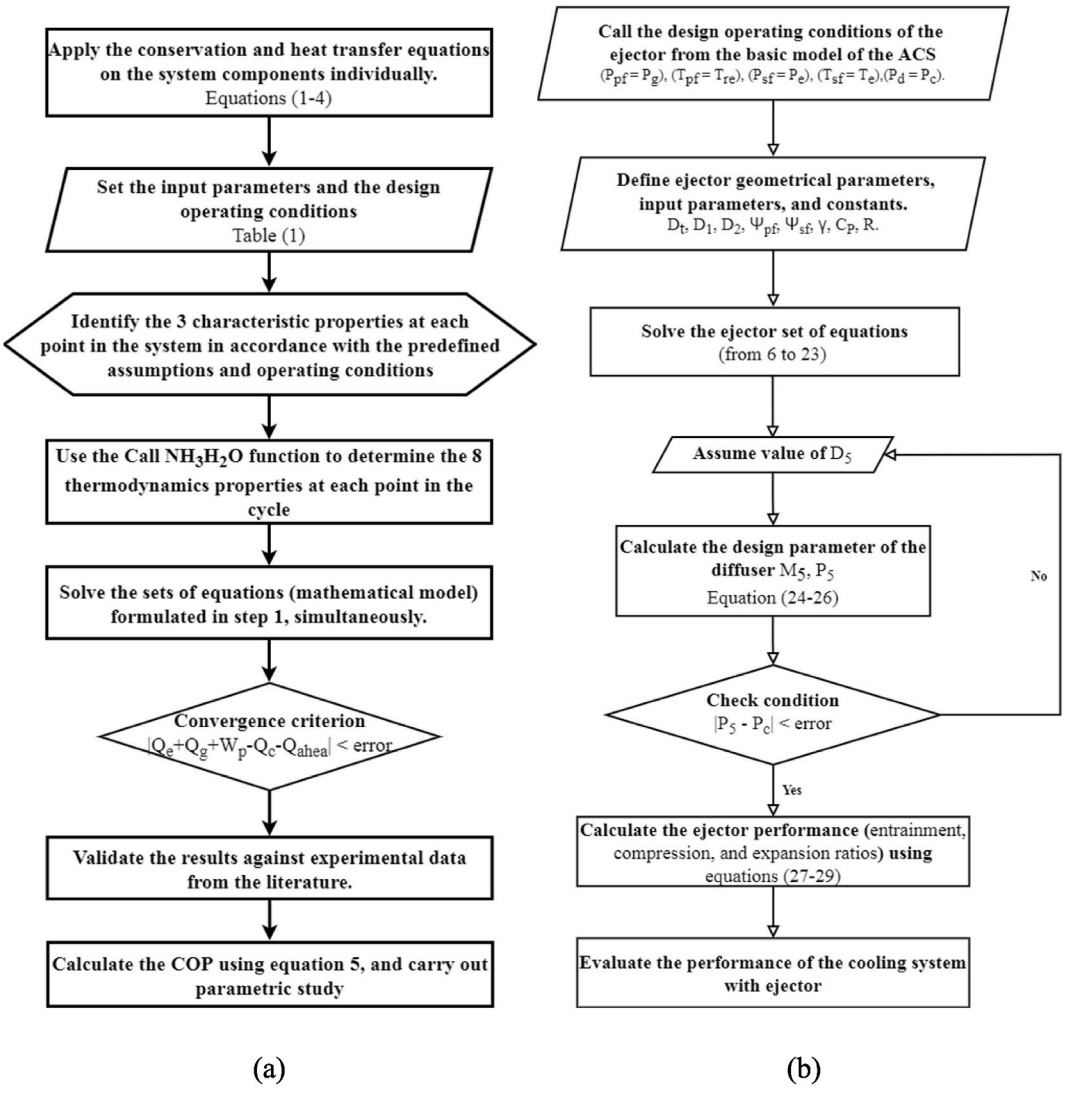

Fig. 4. Solution algorithm of (a) RACS model (b) ejector model.

Table 3
Model validation against experimental and theoretical data reported in Ref. [17].

Point	Experimental data [17] (Average values)	Theoretical model [17]	Current model	Deviation of Araujo et al. model from experimental data [17]	Deviation of the current model from experimental data
1	348.43	330.42	369.6	5.2%	6.1%
2	311.18	314.65	310.2	1.1%	0.3%
3	310.31	311.16	306.4	0.3%	1.3%
4	300.66	283.54	286.8	5.7%	4.6%
5	281.63	280.31	276.2	0.5%	1.9%
6	285.85	281.85	281.85	1.4%	1.4%
7	285.72	306.18	321.5	7.2%	12.5%
8	341.80	340.58	352.0	0.4%	3.0%
9	313.60	314.65	308.65	0.3%	1.6%
10	315.30	314.85	308.7	0.1%	2.1%
11	343.27	320.70	360.3	6.6%	5.0%
12	378.90	337.50	364.6	10.9%	3.8%
13	399.51	380.45	399.6	4.8%	0.0%
14	398.20	349.33	367.4	12.3%	7.7%
15	379.33	355.03	394.6	6.4%	4.0%
16	366.17	355.14	379.6	3.0%	3.7%

*All temperatures are in Kelvin.

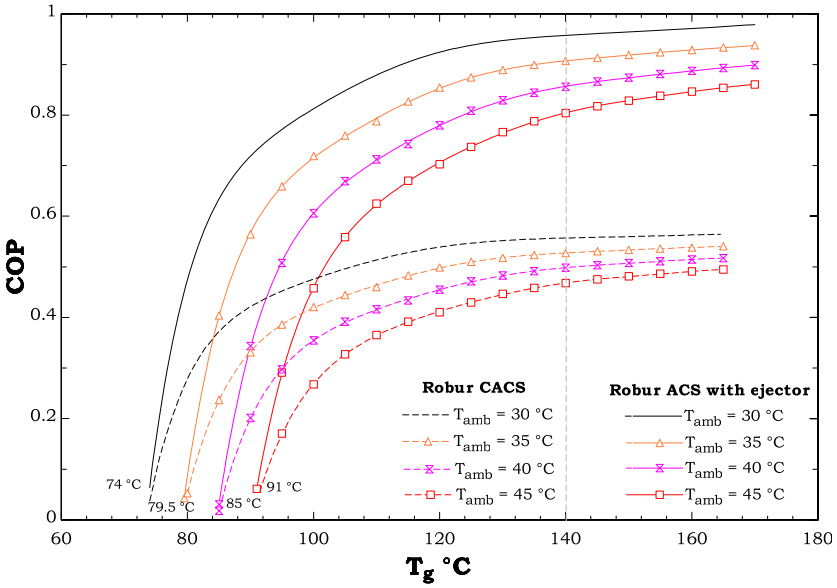

Fig. 5. COP trend with generator temperature (T_g) at different ambient temperatures (T_{amb}).

ammonia dissolved in the solution that exists in the generator. As the generator temperature rises, more refrigerant vapor is generated and the CR declines sharply. Thereafter, the generator becomes incapable to generate much more refrigerant, and the absorbent (water) vaporizes excessively. Eventually, at higher temperatures (over 120 °C) the CR approximately becomes unchanged. This trend is similar for all ambient temperatures as presented in Fig. 6(b).

The commercial unit under study is designed for chilled water output temperature of above 0 °C. The evaporator pressure is determined by the manufacturer not to be less than 4 bar [18]. Accordingly, the least operating temperature of the evaporator is limited to 4 °C. The effect of the evaporator pressure on the COP and the CR was examined and the result is depicted in Fig. 7. The COP value increased gradually with the evaporator pressure until it reached a peak, hence it started to decline. Under all tested ambient temperatures, the peak was obtained at around 5 bar. Thus, for typical air conditioning purposes, it is recommended to set the lower pressure at 5 bar.

The ambient temperature affects the minimum operating evaporator pressure. At 45 °C ambient temperature, the system is incapable to operate at a lower pressure of 4 bar. Hence, the minimum operating pressure at the evaporator is raised to 4.1 bar. However, in this case, the CR will be as high as 20.2 (Fig. 7).

The ejector specifications adopted in this study were taken from the model as developed by S. Khalili and Farshi [16]. Fig. 8 shows the effect of the throat and mixing tube diameters on the COP. The COP is inversely proportional to the throat diameter. Nevertheless, the minimum throat diameter is limited by the critical choke mode. On the other hand, the COP and the entrainment ratio have an approximately linear proportional relation with the diameter of the mixing tube.

What distinguishes RACS from conventional ACS are the heat recovery processes in the rectifier coil, the absorber coil, and the refrigerant heat exchanger (RHE). The latter was investigated in various studies and showed slight enhancement in the system performance [5]. The heat recovered in the RHE and the absorber coil is presented in Fig. 9 for different ambient temperatures.

At high generator temperatures (above 120 °C), the weak solution exits the generator with high thermal energy content. Hence, the rate of heat transfer to the strong solution inside the absorber coil increases. Concurrently, the rate of heat transfer from the regenerated vapor to the strong solution inside the rectifier coil increases. Nevertheless, the rates of heat transfer are different in the two coils. The heat transfer medium in the absorber coil is the weak ammonia-water solution with a high specific heat capacity. Whereas, the heat transfer medium in the rectifier coil is mainly the regenerated ammonia vapor with a lower specific heat capacity. Therefore, the increment in the rate of recovered heat with the generator temperature was higher in the absorber coil than in the rectifier coil.

To recover the heat wherever there is great potential, three heat exchangers were added to the conventional cycle in the Robur cooling system. Technically, the greater the effectiveness of the heat exchanger the higher the heat recovery rate, consequently, the greater the COP value. This phenomenon is clearly observed in Fig. 10.

Nevertheless, each of these heat exchangers has a different significance on the COP. Abid et al. [5] concluded that the use of RHE enhances the system performance by an order of 4–8%. In the present study, using RHE that hypothetically recovers the whole available heat ($\varepsilon_{RHE} = 1$) would increase the COP by only 6.74% compared to the system without RHE. Whereas, the sensitivity of the COP to the effectiveness of the absorber coil is greater, particularly at high generator temperatures. For instance, at $T_g = 140$ °C, introducing an absorber coil with an effectiveness of 0.6 improves the COP by about 12%. The improvement percentage reaches up to about 21.6% if all available heat is recovered. It should be noted that the data of each curve were obtained at the design operating conditions as detailed in Table 1. The addressed parameter (ε_{abC} or ε_{RHE}) was varied while all other parameters (effectiveness of the other heat exchangers, ejector geometrical parameters, cycle operating pressures and temperatures) were fixed to the design

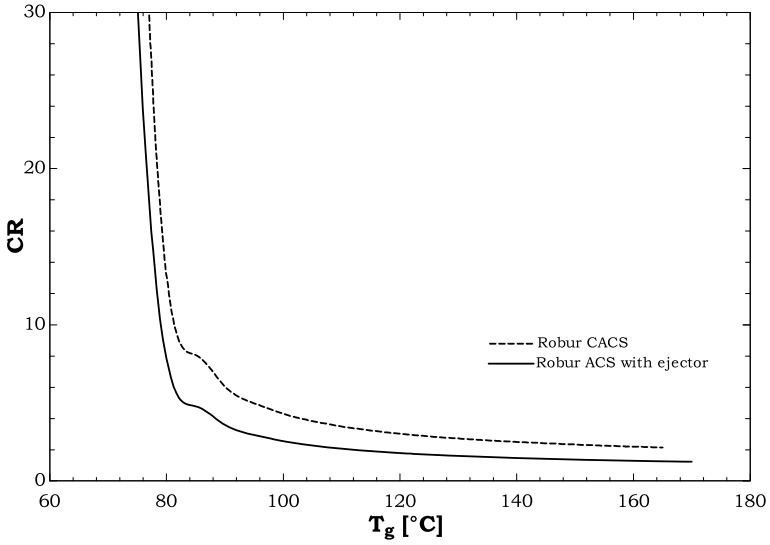

(a) Comparison between conventional and modified RACS.

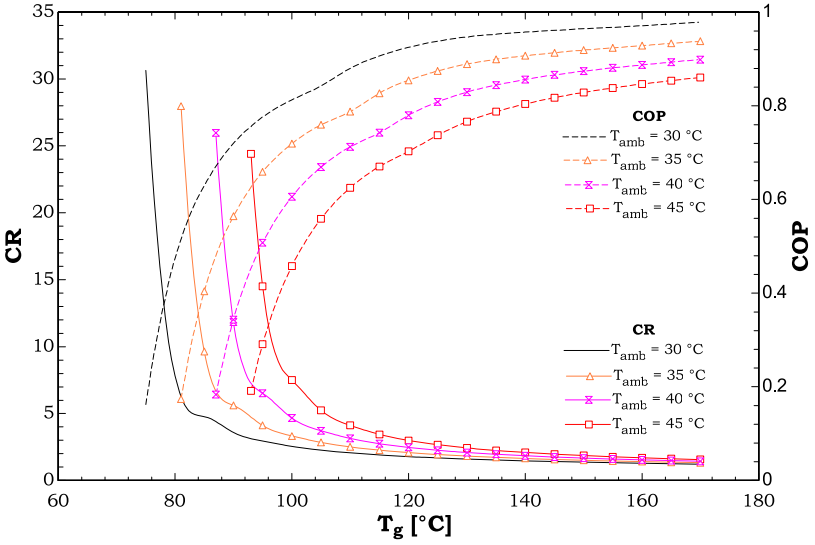

(b) Performance of the modified RACS at different ambient temperatures (T_{amb}).

Fig. 6. Change of the circulation ratio (CR) with the generator temperature (T_g).

conditions. The two curves are depicted in Fig. 10 for comparison purposes.

5. Conclusions

In this study, a mathematical model was developed to describe the performance of the commercially available Robur® absorption cooling system (RACS). The model was based on the mass, concentration, and energy balance equations, in addition to heat transfer equations. The validation of the model results against experimental data available in the literature revealed good agreement, within a maximum deviation of 7.7%. Moreover, the COP of the conventional RACS ranged between 0.4 and 0.56, which corresponded to the results obtained by the experiment of Araujo et al. [17].

Furthermore, to improve the performance of the commercial chiller, the use of an ejector was proposed. A vapor-vapor ejector was introduced between the generator and the condenser, such that a triple pressure levels absorption cooling system was configured. The vapor-vapor ejector was modeled based on gas dynamics equations, in addition to the shock circle method. The performance of the RACS before and after adding the ejector was compared in terms of the coefficient of performance (COP), and the circulation ratio (CR). The former indicates the technical performance of the chiller, while the latter relates to the size of the system. At the design conditions, the modified system achieved a COP of 0.81, which represented an improvement of 70.6% over the COP of the

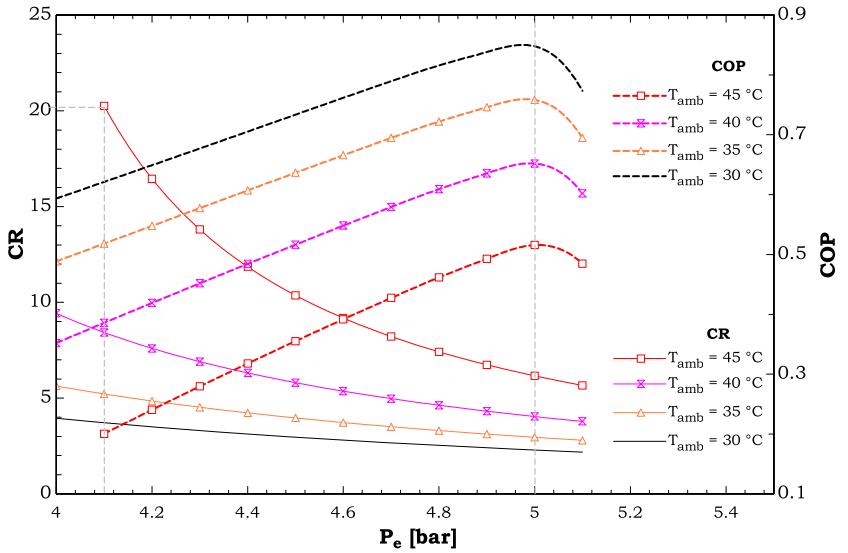

Fig. 7. Change in CR and COP with evaporator pressure (P_e) at different T_{amb}.

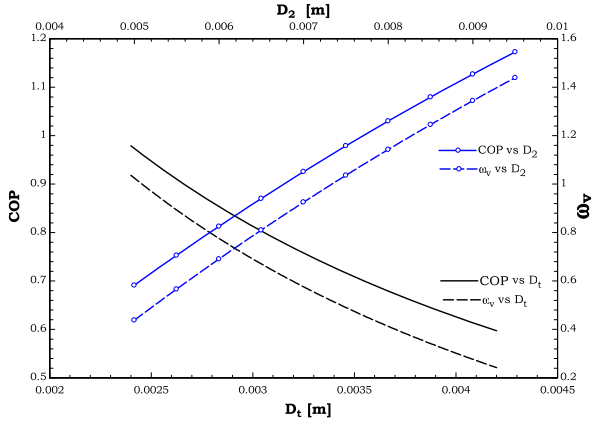

Fig. 8. Effects of the throat diameter (D_t) and the mixing tube diameter (D_2) on the COP and the entrainment ratio (ω_v).

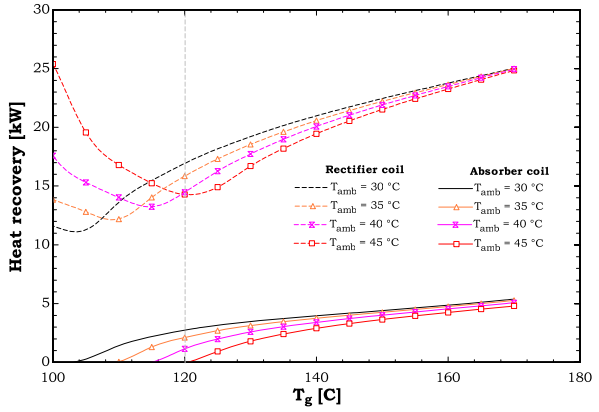

Fig. 9. Heat recovered in the rectifier and absorber coils at different generator temperatures (T_g) under different ambient temperatures (T_{amb}).

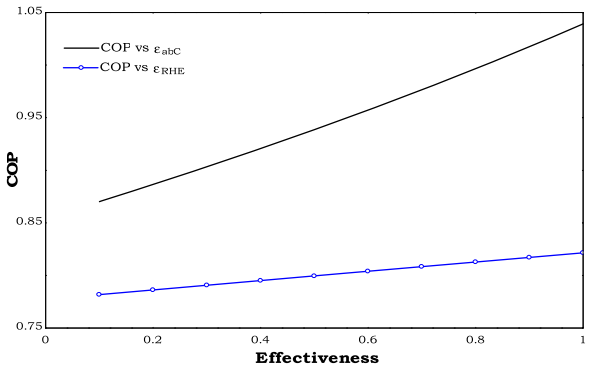

Fig. 10. Sensitivity of the COP to the effectiveness of absorber coil (ε_{abC}) and RHE (ε_{RHE}) at ($T_g = 140\ ^\circ C$, $T_{amb} = 30\ ^\circ C$, $T_e = 5\ ^\circ C$).

conventional RACS. Moreover, the results showed that the utilization of the ejector decreased the CR by 41% on average.

A parametric study was carried for the modified system. As the commercial RACS is an air cooled system, the effect of the surrounding ambient temperature was of great impact. It was found that the increase in the ambient temperature decreased the COP and increased the CR and the minimum required temperature inside the generator (the activation temperature). The COP value increased with the increase in generator temperature. However, the rate of the increment decreased significantly above 130 °C. Further increasing in the generator temperature slightly improved the performance, but it would increase the heat loss to the surrounding. In warmer environments, it is recommended to operate the evaporator at relatively higher pressures to avoid the need for high circulation ratios.

The system performance was further enhanced by decreasing the ejector throat diameter, and increasing the mixing-tube diameter. However, any change in these dimensions is conditioned by fulfilling the chock mode and the shock wave that are only obtainable within a specific range of operating conditions. Practically, it is difficult to control the operating conditions of the ejector. Therefore, utilizing ejectors with adjustable nozzle-positions is recommended.

The heat recovery processes characteristics of the RACS were studied. At higher generator temperatures (above 120 °C), the increment in the rate of heat recovery in the absorber coil was higher than in the rectifier coil. The difference was caused by the nature of the heat transfer medium in each coil. It was found that the COP sensitivity to the effectiveness of the absorber coil was greater than to the effectiveness of the RHE, particularly at high generator temperatures.

Funding

The work in this paper was funded by Qatar National Research Fund under its National Priorities Research Program [Award number NPRP11S-0114-180295]. The contents of this work are solely the responsibility of the authors and do not necessarily represent the official views of the Qatar National Research Fund. Open Access funding was supported by the Qatar National Library.

Author contributions

Hamza K. Mukhtar: Conceptualization, Methodology, Data curation, Software, Visualization, Writing- Original draft preparation. Saud Ghani: Conceptualization, Formal analysis, Supervision, Writing- Reviewing and Editing.

Declaration of competing interest

The authors declare that they have no known competing financial interests or personal relationships that could have appeared to influence the work reported in this paper.

Data availability

Data will be made available on request.

Acknowledgement

The authors would like to acknowledge Qatar National Research Fund, and Qatar National Library for their financial support.

References

[1] O. Rejeb, C. Ghenai, M. Bettayeb, Modeling and simulation analysis of solar absorption chiller driven by nanofluid-based parabolic trough collectors (PTC) under hot climatic conditions, Case Stud. Therm. Eng. 19 (2020), 100624, https://doi.org/10.1016/j.csite.2020.100624. February.

[2] J.M. Labus, C.C. Bruno, A. Coronas, Review on absorption technology with emphasis on small capacity absorption machines, Therm. Sci. 17 (3) (2013) 739–762, https://doi.org/10.2298/TSCI120319016L.

[3] N.A. Darwish, S.H. Al-Hashimi, A.S. Al-Mansoori, Performance analysis and evaluation of a commercial absorption-refrigeration water-ammonia (ARWA) system, Int. J. Refrig. 31 (7) (2008) 1214–1223, https://doi.org/10.1016/j.ijrefrig.2008.02.005.
[4] H.M. Ali, H. Ali, M. Abubaker, A. Saieed, W. Pao, M. Ahmadlouydarab, H. Koten, M. Abid, Condensate retention as a function of condensate flow rate on horizontal enhanced pin-fin tubes, Therm. Sci. (6) (2018) 3887–3892, https://doi.org/10.2298/TSCI171129161A, 2018.
[5] A.M. Abed, M.A. Alghoul, K. Sopian, H.S. Majdi, A.N. Al-Shamani, A.F. Muftah, Enhancement aspects of single stage absorption cooling cycle: a detailed review, Renew. Sustain. Energy Rev. 77 (2017), https://doi.org/10.1016/j.rser.2016.11.231.
[6] I. Horuz, T.M.S. Callander, Experimental investigation of a vapor absorption refrigeration system, Int. J. Refrig. 27 (1) (2004) 10–16, https://doi.org/10.1016/S0140-7007(03)00119-1.
[7] R.M. Lazzarin, A. Gasparella, G.A. Longo, Ammonia-water absorption machines for refrigeration: theoretical and real performances, Int. J. Refrig. 19 (4) (1996) 239–246, https://doi.org/10.1016/0140-7007(96)00016-3.
[8] R. Mansouri, I. Boukholda, M. Bourouis, A. Bellagi, Modelling and testing the performance of a commercial ammonia/water absorption chiller using Aspen-Plus platform, Energy 93 (2) (2015) 2374–2383, https://doi.org/10.1016/j.energy.2015.10.081.
[9] A. Häberle, F. Luginsland, C. Zahler, M. Berger, M. Rommel, H.M. Henning, A linear concentrating Fresnel collector driving a NH3 – H2O absorption chiller,, in: Proc. Second Int. Conf. Sol. Air-Conditioning, Tarragona, Spain, 2007, pp. 662–667.
[10] C. Weber, M. Berger, F. Mehling, A. Heinrich, T. Núñez, Solar cooling with water-ammonia absorption chillers and concentrating solar collector - operational experience, Int. J. Refrig. 39 (2014) 57–76, https://doi.org/10.1016/j.ijrefrig.2013.08.022.
[11] H.K. Mukhtar, S. Ghani, Hybrid ejector-absorption refrigeration systems: a review, Energies 14 (2021) 20, https://doi.org/10.3390/en14206576.
[12] Y. Zhu, W. Cai, C. Wen, Y. Li, Shock circle model for ejector performance evaluation, Energy Convers. Manag. 48 (9) (2007) 2533–2541, https://doi.org/10.1016/j.enconman.2007.03.024.
[13] M. Cefarin Commissione, "Design of Nh 3-H 2 O Absorption Chiller for Low Grade Waste Heat Recovery.".
[14] F.A. Boyaghchi, M. Mahmoodnezhad, V. Sabeti, Exergoeconomic analysis and optimization of a solar driven dual-evaporator vapor compression-absorption cascade refrigeration system using water/CuO nanofluid, J. Clean. Prod. 139 (2016) 970–985, https://doi.org/10.1016/j.jclepro.2016.08.125.
[15] C. Vereda, R. Ventas, A. Lecuona, M. Venegas, Study of an ejector-absorption refrigeration cycle with an adaptable ejector nozzle for different working conditions, Appl. Energy 97 (2012) 305–312, https://doi.org/10.1016/j.apenergy.2011.12.070.
[16] S. Khalili, L. Garousi Farshi, Design and performance evaluation of a double ejector boosted multi-pressure level absorption cycle for refrigeration, Sustain. Energy Technol. Assessments 42 (Dec) (2020), https://doi.org/10.1016/j.seta.2020.100836.
[17] J.J.P. de Araújo, C.A.C. dos Santos, C.A.M. de Holanda, J.B.F. Duarte, A.A.O. Villa, J.C.C. Dutra, Energetic analysis of a commercial absorption refrigeration unit using an ammonia-water mixture, Acta Sci. Technol. 39 (4) (2017) 439–448, https://doi.org/10.4025/actascitechnol.v39i4.29904.
[18] Robur Corporation, Installation, Use and Maintenance Manual GA Line ACF 60-00 Model, 2017 [Online]. Available: https://www.performanceengineering.com/cm/dpl/downloads/content/509/Install_Instructions.pdf.